Chemical Bubble Dynamics and Quantitative Sonochemistry

A. J. Colussi,* Linda K. Weavers, and Michael R. Hoffmann*

Environmental Engineering Science, California Institute of Technology, Pasadena, California 91125

Received: January 28, 1998; In Final Form: June 12, 1998

We model the collapse of a bubble by taking into account all the energy forms involved (i.e., mechanical, thermal, chemical, and radiative) and compare the calculated radical yields with sonochemical data in H_2O. Water decomposition plays a critical role in the energy balance, but trails equilibrium even in bubbles collapsing at subsonic speeds. Integration of the equation of bubble motion coupled with a full chemical mechanism reveals that (1) terminal gas temperatures and Mach numbers M_L increase in cooler water, (2) Γ_{OH}, the number of OH-radicals produced per unit applied work at maximum M_L—when bubbles become unstable and disperse into the liquid—decreases at small *and* very large sound intensities. We show that available data on the sonochemical decomposition of volatile solutes—such as CCl_4, which is pyrolyzed within collapsing bubbles—are compatible with the efficient conversion of ultrasonic energy into transient cavitation. On this basis we calculate $\Gamma_{OH} = (1 \pm 0.5) \times 10^{17}$ molecules/J for $R_0 = 2$ μm bubbles optimally sonicated at 300 kHz and 2.3 W/cm^2 by assuming mass and energy accommodation coefficients of $\alpha \leq 7 \times 10^{-3}$ and $\epsilon \leq 0.04$, respectively, in gas−liquid collisions, and values about 3-fold smaller after averaging over the nuclei size distribution. Since there is negligible radical recombination during dispersal, these Γ_{OH} values represent available oxidant yields, that agree with experimental data on iodide sonochemical oxidation. Bubbles emit little radiation, suggesting that only radial shock waves may heat small regions to the 10^4-10^5 K range required by some sonoluminescence experiments. The contribution of this sonoluminescent core to sonochemical action is, however, insignificant. We show that much larger accommodation coefficients would lead to higher temperatures, but also to O atoms rather than OH radicals and ultimately to excess O_2, at variance with experimental evidence.

Introduction

Liquids exposed to ultrasound emit radiation and undergo chemical decomposition.[1−4] It is generally agreed that both phenomena take place during the sudden collapse of bubbles generated by acoustical expansion of preexisting gas nuclei.[4a] Inferred maximum temperatures, T_{max}, range from 3 to 50 kK, depending on the specific experimental probe.[5−7] For example, chemical effects are compatible with temperatures at the lower end of the range,[7] while discrete emissions from excited OH, C_2, and CN species require temperatures above ca. 6 kK.[6] On the other hand, the intense sonoluminescence spikes observed under certain conditions are associated with blackbody radiation sources emitting over the range 25−50 kK.[8−12] Currently, it is unknown whether these widely different temperatures apply to dissimilar domains or portray successive stages of identical loci. One may also wish to control these outcomes and the energy efficiency of sonochemical experiments.

The dynamics of bubble collapse is determined by energy conservation during the conversion of external work into kinetic energy of the liquid shell, heat content of the gases, chemical reaction enthalpy, emitted radiation, and heat lost into the liquid.[13−15] In this paper we show, for the first time, that the endothermic atomization of solvent molecules represents a major contribution to the energy balance of the bubble and actually controls the last phase of collapse. The explicit incorporation of chemical enthalpy changes into the equation of bubble motion rationalizes the complex, and sometimes puzzling, effects associated with acoustic cavitation in liquids.[10c] We evaluate the energy efficiency of sonochemical action and estimate decomposition rates of volatile and nonvolatile solutes in aqueous media that closely agree with reported experimental data.[16−19] The emerging view is that sonochemistry and sonoluminiscence are related but complementary manifestations of nonequilibrium phenomena inextricably linked to chemical reaction rates and energies.

Modeling the Adiabatic Compression of a Reactive Bubble

Let R_0 and R_{max} be the equilibrium and maximum radii, respectively, of a spherical gas bubble subjected to an acoustic field of frequency f (in kHz) and amplitude P_a (in atm; 1 atm $= 10^5$ Pa).[14a] These wave parameters will be denoted as (f, P_a). Pressure amplitude is related to acoustic intensity I_a by $P_a = (2\rho c_L I_a)^{1/2}$, where ρ and c_L stand for the medium density and speed of sound, respectively.[4a] The equilibrium gas (assumed to be argon unless otherwise indicated) pressure inside the initial bubble is given by $P_{g,e} = P_0 - P_{vap} + 2\sigma/R_0$, where P_0 is the hydrostatic pressure, $P_{vap} = 3.0$ kPa is the vapor pressure of the liquid, and $\sigma = 0.072$ N m^{-1} is its surface tension at 300 K. Since during the slow isothermal expansion gas pressure drops by a factor $z = (R_{max}/R_0)^3$, while P_{vap} is assumed to remain constant, the composition of the gas at R_{max} is a sensitive function of z. For instance, if $P_{g,e} \sim 1$ atm, even a modest ratio $R_{max}/R_0 \sim 3.2$, $z = 32.8$, leads to a 1:1 H_2O/Ar mixture in the expanded bubble.

Starting at $R = R_{max}$, $dR/dt = R'(0) = 0$, the bubble contracts under an external pressure $P_{ext} = P_0 + \varphi P_a$, where $\varphi P_a = \int_{-t\,exp}^{t} \sin(2\pi f t')\, d(t'/t)$ is the effective acoustic pressure at time

S1089-5639(98)00930-X CCC: $15.00
Published on Web 08/11/1998

TABLE 1: Reaction Rate Constants[1] (in molecule cm^{-3}, s Units, as Applicable)

reaction	rate constants[a] (in molecule cm^{-3}, s units, as applicable)
$H_2O + M \leftrightarrow H + OH + M$ (7,−7)	$k_7 = 5.8E{-}9 \exp(-52900/T)$;[b] $k_{-7} = 6.1E{-}26\ T^{-2}$
$OH + M \leftrightarrow O + H + M$ (8,−8)	$k_8 = 4.0E{-}9 \exp(-50000/T)$; $k_{-8} = 1.3E{-}29\ T^{-1}$
$H_2O + H \leftrightarrow OH + H_2$ (9,−9)	$k_9 = 1.0E{-}16\ T^{1.9} \exp(-9265/T)$; $k_{-9} = 1.1E{-}17\ T^{2} \exp(-1490/T)$
$2OH \leftrightarrow O + H_2O$ (10,−10)	$k_{10} = 3.5E{-}16\ T^{1.4} \exp(200/T)$; $k_{-10} = 7.6E{-}15\ T^{1.3} \exp(-8605/T)$
$O + OH \leftrightarrow O_2 + H$ (11,−11)	$k_{11} = 7.5E{-}10\ T^{-1/2} \exp(-30/T)$; $k_{-11} = 5.9E{-}8\ T^{-0.7} \exp(-8569/T)$
$2O + M \leftrightarrow O_2 + M$ (12,−12)	$k_{12} = 5.2E{-}35 \exp(900/T)$; $k_{-12} = 3.0E{-}6\ T^{-1} \exp(-59429/T)$
$2OH + M \leftrightarrow H_2O_2 + M$ (13,−13)	$k_{13} = 1.6E{-}23\ T^{-3}$; $k_{-13} = 2.1e9\ T^{-4.86} \exp(-26795/T)$
$H + O_2 + M \leftrightarrow HO_2 + M$ (14,−14)	$k_{14} = 1.8E{-}29\ T^{-1}$; $k_{-14} = 2E{-}5\ T^{-1.18} \exp(-24363/T)$
$2HO_2 \rightarrow H_2O_2 + O_2$ (15,−15)	$k_{15} = 3.0E{-}12$; $k_{-15} = 9.0E{-}11 \exp(-20000/T)$
$2H + M \leftrightarrow H_2 + M$ (16,−16)	$k_{16} = 1.5E{-}29\ T^{-1.3}$; $k_{-16} = 7.6E{-}5\ T^{-1.4} \exp(-52530/T)$
$O + H_2 \leftrightarrow OH + H$ (17,−17)	$k_{17} = 2.5E{-}11\ T^{2.0} \exp(-3801/T)$; $k_{-17} = 8.1E{-}21\ T^{2.8} \exp(-1950/T)$
$HO_2 + O \leftrightarrow OH + O_2$ (18,−18)	$k_{18} = 2.9E{-}11 \exp(200/T)$; $k_{-18} = 3.7E{-}11 \exp(-26500/T)$
$H + HO_2 \rightarrow 2OH$ (19)	$k_{19} = 2.8E{-}10 \exp(-440/T)$
$HO_2 + OH \rightarrow H_2O + O_2$ (20)	$k_{20} = 2.4E{-}8\ T^{-1}$
$H + H_2O_2 \leftrightarrow HO_2 + H_2$ (21,−21)	$k_{21} = 8.0E{-}11 \exp(-4000/T)$; $k_{-21} = 5.0E{-}11 \exp(-13100/T)$
$OH + H_2O_2 \rightarrow H_2O + HO_2$ (22)	$k_{22} = 2.9E{-}12 \exp(-160/T)$
$H + HO_2 \leftrightarrow H_2 + O_2$ (23,−23)	$k_{23} = 1.1\ E{-}10 \exp(-1070/T)$; $k_{-23} = 2.4E{-}10 \exp(-28500/T)$
$H + HO_2 \rightarrow H_2O + O$ (24)	$k_{24} = 9.1E{-}11 \exp(-914/T)$
$H_2O_2 + H \rightarrow H_2O + OH$ (25)	$k_{25} = 4.1E{-}11 \exp(-2000/T)$
$O + H_2O_2 \rightarrow OH + HO_2$ (26)	$k_{26} = 1.6E{-}17\ T^{2} \exp(-2000/T)$
$O + O_2 + M \leftrightarrow O_3 + M$ (27,−27)	$k_{27} = 4.0E{-}32/T$; $k_{-27} = 7.2E{-}10 \exp(-11172/T)$
$O + O_3 \rightarrow 2O_2$ (28)	$k_{28} = 8.0E{-}12 \exp(-2060/T)$
$H + O_3 \rightarrow OH + O_2$ (29)	$k_{29} = 1.4E{-}10 \exp(-480/T)$
$OH + O_3 \rightarrow HO_2 + O_2$ (30)	$k_{30} = 1.9E{-}12 \exp(-1000/T)$
$HO_2 + O_3 \rightarrow OH + 2O_2$ (31)	$k_{31} = 1.4E{-}14 \exp(-600/T)$

[a] From refs 20 and 21. [b] Read 5.89E−9 as 5.8×10^{-9}.

t [notice that the integration spans the entire lifetime of the bubble from the onset of expansion at $(-t_{exp})$ and that in general $\varphi P_a(t > 0) > 0$]. Since the 25 μs half-period of a 20 kHz wave is much longer than typical collapse times of a few μs, we will assume that P_{ext} remains nearly constant throughout. This approximation works well even at higher frequencies because collapse times are proportionally shorter. Therefore, the external work done by the liquid on a contracted cavity of radius R is given by

$$W_{ext} = 4\pi P_{ext}({R_{max}}^3 - R^3)/3 + 4\pi\sigma({R_{max}}^2 - R^2) \quad (1)$$

The external work W_{ext}, minus any heat H_d dissipated into the liquid *during* collapse, must be converted into convective kinetic energy of the liquid shell KE_{liq}, plus compression work W_g performed on the bubble gas:

$$W_{ext} - H_d = KE_{liq} + W_g = 2\pi R^3 \rho R'^2 + W_g \quad (2)$$

($KE_{liq} = 2\pi R^3 \rho R'^2$, for an incompressible liquid).[14a,15a] On the other hand, the power delivered to the gas is given by

$$dW_g/dt = -P_g\, dV/dt = -[\delta k_B T/(1 - b\delta)]4\pi R^2 R' \quad (3)$$

($R' < 0$) where P_g is the instantaneous total gas pressure inside and just outside the bubble, δ is the gas density, k_B is Boltzmann's constant, T is the local temperature, and $b = 3.05 \times 10^{-2}$ M^{-1} is the van der Waals constant of H_2O. This work results in the heating of the gas *and the concomitant chemical composition changes*, i.e.,

$$W_g = H_g + Q \quad (4)$$

The heat term, $H_g = n\langle C_v\rangle(T - T_{amb})$, and the chemical energy term, $Q = \sum\langle\Delta H_{fi}\rangle(n_i - n_{io})$, can be evaluated from the instantaneous chemical composition of the mixture and its temperature. The n's stand for number of molecules: $n = \sum n_i$, $n_{io} = n_i(0)$. $\langle C_v\rangle = k_B/(\gamma - 1)$ is the average molecular heat capacity of the mixture, $\gamma = C_p/C_v$, and $\langle\Delta H_{fi}\rangle$ is the heat of formation of species i in J/molecule. We use temperature independent $\langle\Delta H_{fi}\rangle$ and $\langle\gamma\rangle$ values calculated at 2000 K, i.e., about the midpoint of working temperature intervals. For example, for $P_{g,e} = 1$ atm, $R_{max}/R = 10$, i.e., $z = 1 \times 10^3$ at 298 K, the polytropic index $\gamma = (1.67 \times 1 \times 10^{-3} + 1.33 \times 3 \times 10^{-2})/3.1 \times 10^{-2} = 1.34$, is considerably smaller than $\gamma = 1.66$ for neat Ar. A similar bubble under 1 atm O_2 ($\gamma = 1.40$) has $\gamma = 1.33$; that is, γ does not depend appreciably on the nature of the noncondensable gas, provided that $z > 10$. Water vapor losses out of the bubble during the early phase of collapse may slightly increase γ values over those calculated at R_{max} (see below). Hence, from eq 4, with $T_{amb} = 300$ K, we get the implicit equation

$$T = 300 + (W_g - Q)(\gamma - 1)/(nk_B) \quad (5)$$

Finally, by combining eqs 1−5 we obtain

$$dR/dt = -\{66.7P_{ext}[(R_{max}/R)^3 - 1] + (146/R)[(R_{max}/R)^2 - 1] - H_d - (2.2 \times 10^{-9}/R^3)[n(T - 300)/(\gamma - 1) + 0.12Q]\}^{1/2} \quad (6)$$

where R's are in μm, time is in μs, P is in atm, and Q and H_d are in J. Equation 6 is applicable to the collapse of spherical bubbles in water. The initial and most important chemical reactions for this system at high temperatures are

$$H_2O \leftrightarrow H + OH \quad (7,-7)$$

$$OH \leftrightarrow O + H \quad (8,-8)$$

These equilibria are followed by all possible reactions among O- and H-containing diatomic (O_2, H_2), triatomic (HO_2, O_3), and tetratomic (H_2O_2) species X_i as given in Table 1. Reaction rates in variable-volume bubbles are calculated as total differentials:

$$d[X_i]/dt = -(\sum r_j) - [X_i](1/V)\, dV/dt \quad (32)$$

where $\sum r_j$ is the sum of elementary chemical reaction rates at constant volume, and $(1/V)\ dV/dt = 3(R'/R)$ is the volumetric term. The appropriate rate constants k_i's are taken from Tsang and Hampson's compilation as reported in the NIST database.[20,21] All unimolecular reactions considered here are in their second-order region under relevant conditions. Hence, their forward (and reverse) rate constants are assumed to be proportional to $\delta_c = \sum[X_i] + 5[H_2O]$ ($X_i \neq H_2O$), a collisionally effective total gas density which assigns a 5-fold larger efficiency to H_2O molecules as collision partners, in accord with current data.[20b]

Water molecules are assumed to be removed from the bubble by collision with the liquid shell at rates proportional to $k_{mt}(\mu s^{-1}) = (\alpha/4)(S/V)\langle c\rangle = 445\alpha(T/300)^{1/2}/R$ (R in μm), where α is the accommodation coefficient for mass transfer, $S/V = 3/R$ is the surface-to-volume ratio, and $\langle c\rangle$ is the average speed of H_2O molecules in the gas phase. An upper limit of $\alpha = 7 \times 10^{-3}$ at 300 K can be obtained from $P_{vap}(H_2O)$ versus T data using the kinetic theory expression for vaporization processes:[14a]

$$P_{vap} = (\pi n_S k_B T/\alpha)\exp(-\Delta H_{vap}/k_B T) \qquad (33)$$

where n_S is the number density of liquid water at the surface and ΔH_{vap} is the enthalpy of vaporization. Equation 33 assumes that any liquid molecule possessing kinetic energy along a perpendicular direction to the gas−liquid interface in excess over ΔH_{vap} vaporizes and that only a fraction α of gas molecules impinging on the liquid surface are trapped due to slow energy dissipation during collision times. It should be emphasized that in the present context (1) α refers to the probability that a H_2O molecule at $T > 300$ K will stick to liquid water at 300 K, and therefore it is expected to be smaller than the equilibrium value derived from eq 33, (2) most of the mass transfer involves water molecules rather than permanent gases, since H_2O is the only species whose concentration exceeds equilibrium values during the initial, and longest, stage of collapse, $R_0 < R < R_{max}$ (see below and Appendix 1).

The term H_d in eq 2 actually comprises heat losses due to viscous dissipation, energy transfer in molecular collisions of hot gases with the liquid, and photon emissions: $H_d = H_v + H_t + H_r$, respectively. As a first approximation we omit the viscosity contribution. The maximum rate of heat transfer in molecular collisions dH_t/dt (in J/μs) can be calculated as (see above)

$$dH_t/dt = 1.86 \times 10^3 \epsilon R^2 (T/300)^{1/2}[H_2O]\langle C_v\rangle(T - 300) \quad (34)$$

(R in μm), where ϵ is the energy accommodation coefficient and $\langle C_v\rangle$ is the average heat capacity of H_2O. This simplified procedure assumes (1) uniform temperature within the bubble, (2) that water vapor is the major component of the gas mixture and, (3) independent collisions, that is, that the mean free path in the gas phase is larger than the bubble radius. At the high pressures prevalent in the final phase of collapse temperature gradients will necessarily develop. As a result, actual thermal power losses may be smaller than those calculated with eq 34. These approximations are ultimately folded in the ϵ values required to match experimental data. Notice that, in contrast with mass transfer, most of the collisional heat transfer occurs in the final stage of collapse [cf. the $(T - 300)$ factor] (see below). Radiative heat transfer rates are calculated from

$$dH_r/dt = 4\pi R^2 \sigma_{SB}(T^4 - 300^4) \qquad (35)$$

where $\sigma_{SB} = 5.67 \times 10^{-8}$ W m^{-2} K^{-4} is Stefan−Boltzmann's

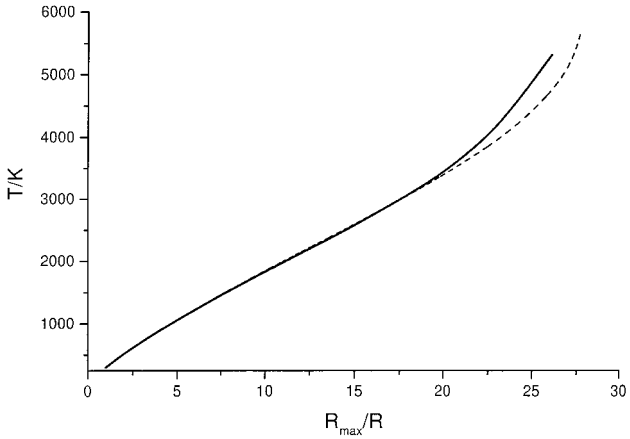

Figure 1. Temperature of collapsing bubbles vs R_{max}/R. $R_0 = 2$ μm and $R_{max} = 28.9$ μm are the equilibrium and maximum bubble radii, respectively. Solid line: bubbles collapsing at $v = 1500$ m/s without chemical reaction. Dashed line: bubbles collapsing at $v = 10$ m/s with chemical reaction (see text).

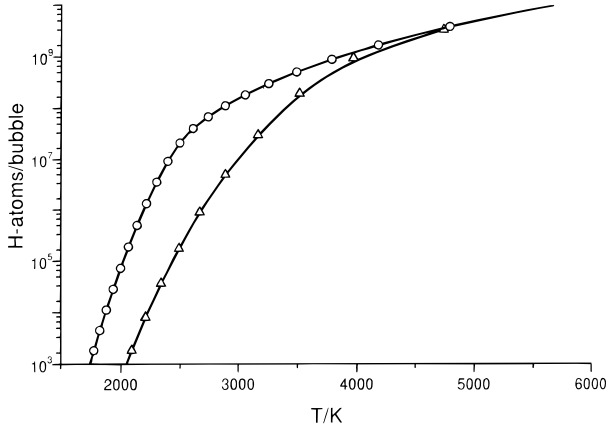

Figure 2. H atom concentration vs temperature in $R_0 = 2$ μm, $R_{max} = 28.9$ μm bubbles collapsing at constant velocity v. Up-triangles and circles: $v = 1500$ and 10 m/s, respectively.

constant. We found that in all cases radiative losses amount to less than a few percent units of W_{ext}. Numerical integration of the resulting sets of algebraic and differential equations was performed with the FACSIMILE program package.[22]

Results and Discussion

The Linearly Collapsing Bubble. It is instructive to begin with the analysis of a bubble contracting at constant velocity v, i.e., $R = R_{max} - vt$, rather than at constant external pressure, to characterize the expected dynamic regimes.[5,6] Notice that the realization of this conceptually simple motion would require a nonsinusoidal acoustic field. Integration of the set of algebraic and differential equations 2−5, plus the corresponding rate expressions 32 for reactions 7, −7 and 8,−8 for $v = 10$, and 1500 m/s, $R_0 = 2\mu$m, $R_{max} = 28.9$ μm, without heat losses, lead to the results shown in Figures 1 and 2. Figure 1 shows the variation of T as a function of R_{max}/R, for ($v = 10$ m/s, with chemical reaction), and ($v = 1500$ m/s, without chemical reaction). The evolution of both systems departs in the last 25% of radial collapse, due to the energy uptake by chemical reaction. Of special interest for the ensuing analysis is the fact that bubble composition depends on v values, Figure 2, implying that finite reaction rates cannot keep up with gas heating even at subsonic speeds (i.e., at Mach numbers $M_L = v/c_L < 1$, where $c_L = 1500$ m/s is the speed of sound in water). Notice that

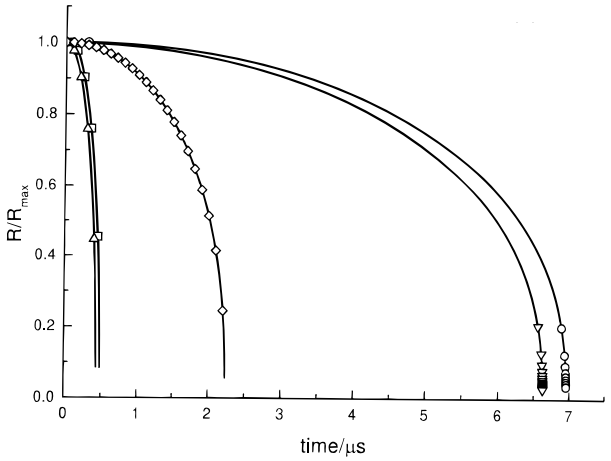

Figure 3. Reduced radii (R/R_{max}) vs time for collapsing bubbles. Circles: $R_0 = 2$ μm; $R_{max} = 128$ μm; $f = 20$ kHz; $P_a = 2$ atm. Down-triangles: the same but with 50% initial water vapor pressure. Diamonds: $R_0 = 2$ μm; $R_{max} = 128$ μm; $f = 300$ kHz; $P_a = 26$ atm. Squares: $R_0 = 2$ μm; $R_{max} = 8.3$ μm; $f = 300$ kHz; $P_a = 2$ atm. Up-triangles: the same but with 50% initial water vapor pressure.

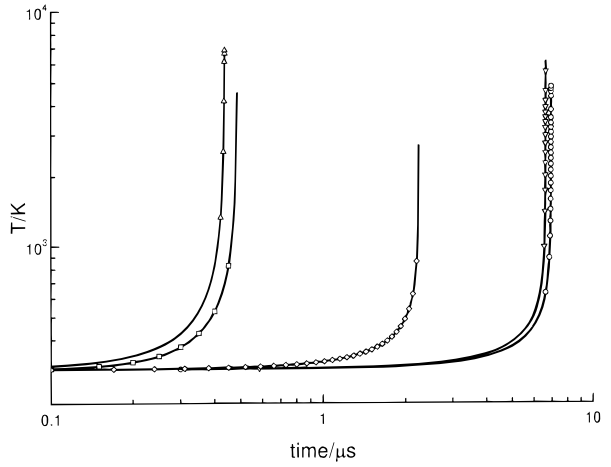

Figure 4. Temperature vs time for the collapsing bubbles of Figure 3.

higher temperatures do not necessarily result in more extensive sonochemical effects because maximum M_L values, i.e., the parameter that controls the point at which bubbles break up, are actually linked to the extent of chemical reactions in real cavities (see below). For example, the number of H atoms at $M_L = 1$, 2500 K, is about 100 times smaller than at $M_L = 6.7 \times 10^{-3}$ (Figure 2), which is very close to the equilibrium value at this temperature.

Collapsing Bubble under Constant External Pressure. The integration of eqs 5−32, for the full reaction mechanism of Table 1, with $R_0 = 2$ μm bubbles excited by (20 kHz, 2 atm) and (300 kHz, 2 and 26 atm) waves, with $\alpha = 0.001$, $\epsilon = 0$, i.e., in truly adiabatic collapses, leads to the results of Figures 3−5. Maximum radii (in μm) were calculated as follows:[4a]

$$R_{max} = (3 \times 10^3/f)(P_a - 1)(P_a)^{-1/2}\,[1 + 2(P_a - 1)/3]^{1/3} \quad (36)$$

where P_a is in atm and f is in kHz. Note that P_a and R_{max} are not independent parameters, and that R_{max} becomes independent of R_0 for bubbles undergoing transient cavitation, i.e., those complying with the condition $R_{max}/R_0 \geq 3$.[14b] Bubble radii evolve as shown in Figure 3. Collapse times vary between 0.4 and 6.6 μs at $P_a = 2$ atm, for $f = 300$, 20 kHz, respectively.

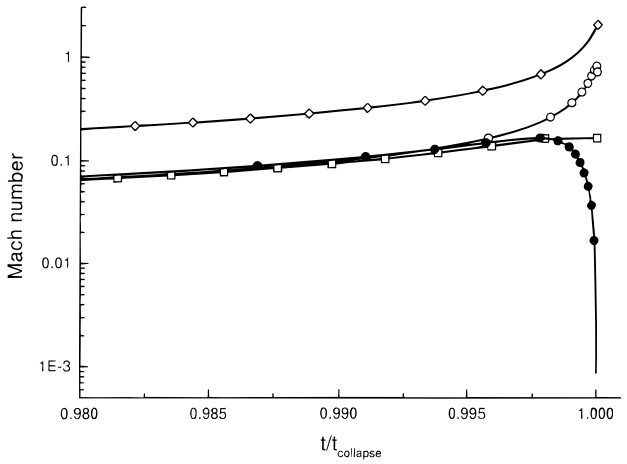

Figure 5. Mach number M_L for the bubble radial velocity relative to the speed of sound in water at 300 K vs the reduced collapse time. Diamonds: $R_0 = 2$ μm; $R_{max} = 128$ μm; $f = 300$ kHz; $P_a = 26$ atm). Open circles: ($R_0 = 2$ μm; $R_{max} = 128$ μm; $f = 20$ kHz; $P_a = 2$ atm. Squares: $R_0 = 2$ μm; $R_{max} = 8.3$ μm; $f = 300$ kHz; $P_a = 2$ atm. Solid circles: the same as squares but without chemical reaction.

We note that a reduction of the initial vapor pressure by a factor of 2 (e.g., cooling the liquid by about 10 °C) results in faster collapses. A $R_0 = 2$ μm bubble expanded to $R_m = 127$ μm by a (300 kHz, $P_a = 26$ atm) wave collapses in 2.3 μs (i.e., a factor of 3 shorter than a similarly expanded bubble by a 20 kHz, 2 atm sonic field). In Figure 4, we show the temperature evolution for each case. The temperature rise is stronger than exponential in all cases. The predicted maximum temperatures are 4810 and 4512 K for 20 and 300 kHz at $P_a = 2$ atm, but rise significantly when water vapor pressure is decreased by 50%, to 6125 and 5128 K, respectively. However, for (300 kHz, 26 atm) the final collapse temperature (2694 K) is predicted to be considerably lower. By removing Q from eqs 5 and 6, we calculate $T_{max} = 6920$ K for (300 kHz, 2 atm); that is, temperatures could rise about 2000 K higher in a chemically inert, fictitious bubble.

Radial velocities display unexpected dependences on experimental parameters. In Figure 5, we show that the maximum velocity, expressed as a Mach number, reaches $M_L = 0.84$ under (20 kHz, 2 atm), but only $M_L = 0.17$ under a 300 kHz wave of the same power. The very energetic collapse at (300 kHz, 26 atm) does become supersonic near the end of the collapse. The remarkable effect of ambient temperature on bubble dynamics is shown in Figure 6. In this case the motion of a collapsing bubble at (20 kHz, 2 atm) becomes supersonic by lowering T_{amb} from 298 to 288 K.[10c] In most runs it is possible to discern the point at which the radial velocity goes through a maximum before sharply falling off. It has been shown that at this stage, where the radial acceleration R'' vanishes, the spherical bubble becomes extremely sensitive to perturbations and breaks up into a cloud of smaller fragments.[15b,c] Since our model applies to a spherical bubble possessing uniform temperatures and pressures (i.e., when molecular velocities are faster than the imploding liquid shell), (1) supersonic Mach numbers merely imply that localized conditions for the development of radial shock waves inside the gas bubbles are met in some cases and (2) our results may not apply beyond $R'' = 0$, because, although an ideal bubble formally rebounds, actual bubbles will burst. We verified that supersonic speeds always develop earlier in the liquid than in the compressed gas, where the speed of sound is a strong function of (T,P).

The inclusion of the chemical energy term in eq 6 seems to provide a possible explanation for the apparent mystery associ-

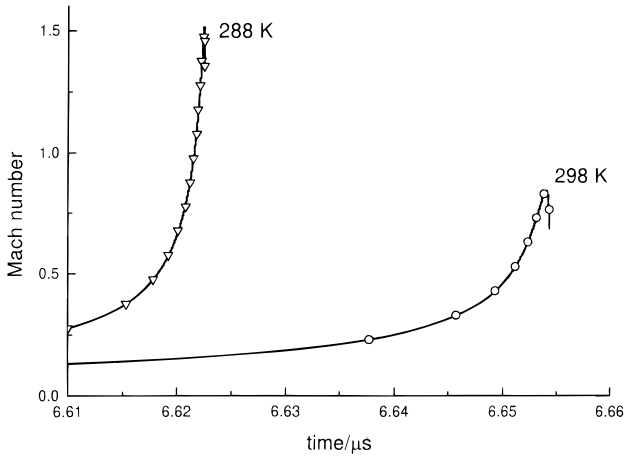

Figure 6. Mach number vs time for collapsing ($R_0 = 2$ μm; $R_{max} = 128$ μm; $f = 20$ kHz; $P_a = 2$ atm) bubbles at 288 and 298 K. A 10 K temperature drops lowers water vapor pressure by a factor of 2.

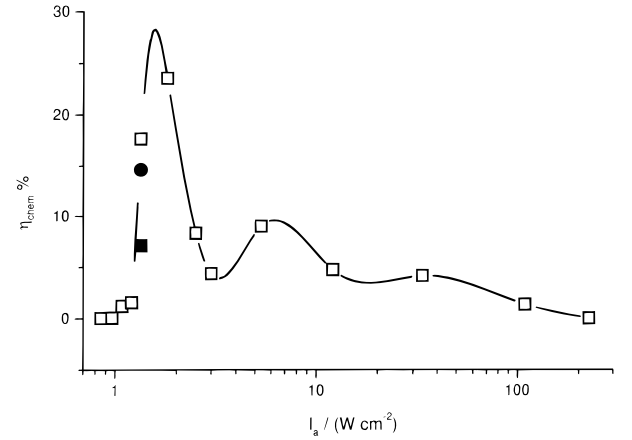

Figure 7. Fraction of acoustic work converted into chemical energy η_{chem} vs absorbed sound intensity I_a for $R_0 = 2$ μm bubbles under $f =$ 300 kHz ultrasound of variable intensity. The solid square corresponds to a bubble containing a 30% O_2/Ar noncondensable gas mixture. The solid circle is for $R_0 = 2$ μm bubbles under a $f = 20$ kHz sonic field.

ated with intense single-bubble sonoluminiscence: not only does water appear to be a unique medium in this regard but cooler water enhances the phenomenon (see above).[10] More complex liquids, such as hydrocarbons, necessarily possess larger atomization energies and, in general, will decompose at lower temperatures than water, preempting the onset of shock waves and extremely high local temperatures. Obvious corollaries of these arguments are that (1) it is impossible to reach uniform temperatures above 10 kK in actual bubbles due to chemical reaction and[8] (2) that the chemical changes taking place in the "hot spots" intensely emitting blackbody radiation are minimal, on account of the infinitesimally small mass involved.

Sonochemical Efficiency. When considering the chemical applications of ultrasound, it is useful to know the efficiency for the conversion of acoustic energy into chemical potential η_{chem}:[1,14b,24]

$$\eta_{chem} = Q/W_{ext} \tag{37}$$

as a function of experimental parameters. In Figure 7 we show results for the excitation of $R_0 = 2$ μm bubbles with 300 kHz ultrasonic waves of variable intensity. η_{chem} increases sharply with power, reaching a maximum of about 28% conversion at $P_a \sim 2.2$ atm. At the same power, the calculated value for 20 kHz is about 50% smaller than at 300 kHz. At larger sound intensities one may get faster bubble wall implosion velocities, higher temperatures, more noise, and better stirring but poorer chemical effects on a relative basis, reflecting the substantial departure from chemical equilibrium conditions within rapidly compressed bubbles. The fact that finite chemical reaction rates cannot keep up with extremely rapid heating profiles must be recognized in the design and analysis of sonochemical experiments.[25,26]

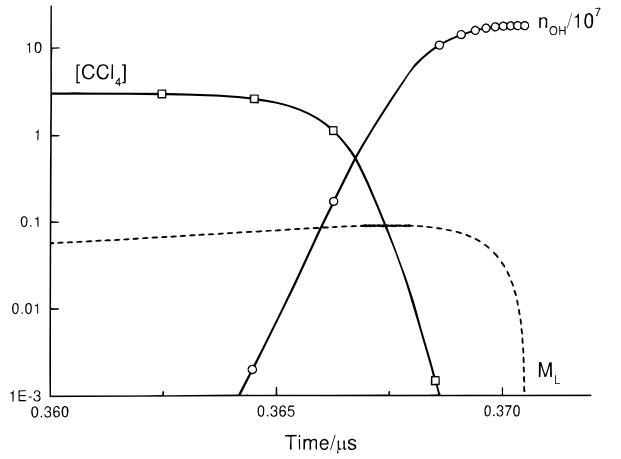

Figure 8. Calculated values for ($R_0 = 2$ μm, $P_a = 1.8$ atm, $f = 300$ kHz, $x_{CCl4} = 0.003$) vs time. n_{OH} in molecules/bubble, [CCl_4] in 10^{17} molecules/cm^3. M_L is the Mach number. CCl_4 decomposition calculated with $k_{38}(s^{-1}) = 2.2 \times 10^{12} \exp(-27727/T)$. Notice that n_{OH} is increasing exponentially during bubble breakup (indicated as a solid segment in the M_L curve).

It is convenient to classify sonochemically reactive solutes into volatile and nonvolatile. The latter can be degraded provided that some of the oxidizing (such as OH, O, HO_2, or H_2O_2) or reducing (such as H or HO_2) species produced in water pyrolysis escape into the solution.[16,27,28] Volatile solutes may decompose thermally (such as CCl_4) and engage in gas-phase radical−molecule reactions (most solutes qualify in this regard) within the bubble.

Let us consider first the case of CCl_4, a surrogate for a volatile and relatively inert-to-radical-attack water contaminant.[18,19] Its equilibrium concentration in the vapor filling the bubble is determined by its Henry's constant ($H = 25$ atm/M for CCl_4 in water at 300 K); that is, the number of CCl_4 molecules per bubble is given by $N_S = \beta H[CCl_4]R_0^3$, where $\beta = 1 \times 10^8$ molecules/(atm μm^3) at 300 K, and [CCl_4] is in M. On the other hand, the energy E_B needed to expand a bubble from R_0 to R_{max} depends on f and P_a, but it is relatively insensitive to R_0, provided that $R_{max}/R_0 > 3$. It can be evaluated from

$$E_B = (4\pi/3)(P_a + P_0)(R_{max}^3 - R_0^3) \sim 4.19 \times 10^{-13}(P_a + P_0)R_{max}^3 \tag{38}$$

where E_B is in J, P_a is in atm and R_{max} is in μm. For example, at (358 kHz, $P_a = 2.48$ atm) we obtain $R_{max} = 10$ μm, and $E_B = 1.4$ nJ/bubble. Hence, the maximum rate at which such bubbles are created by ultrasound of power density Π (in W/cm^3) is N_B (bubbles cm^{-3} s^{-1}) $= \Pi/E_B$. If, as it happens in this case (Figure 8), all N_S molecules decompose irreversibly in a single cavitation event, maximum destruction rates will be given by $r_{-CCl4}(M\ s^{-1}) = N_S N_B = k[CCl_4] = [(\Pi/E_B)\beta H R_0^3/(6 \times 10^{20})][CCl_4]$. Therefore, the experimental value $k(s^{-1}) = 1.1 \times 10^{-3}$ obtained in our laboratory at $\Pi = 0.08$ W/cm^3[,19] implies that the average equilibrium radius of cavitating bubbles is $\langle R_0 \rangle \sim 1.7$ μm. The latter value is quite plausible because it actually

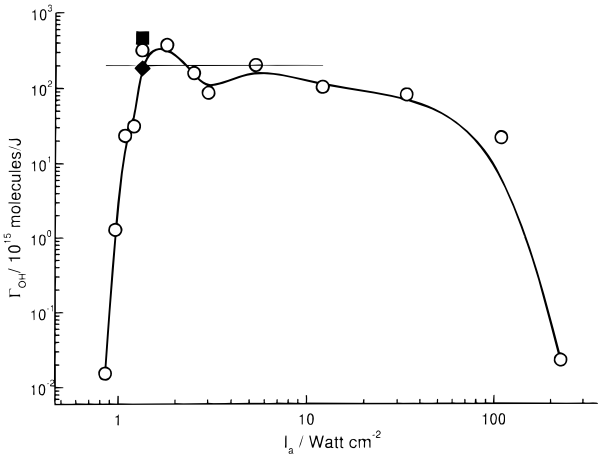

Figure 9. Number of OH radicals produced per bubble per joule at $R'' = 0$: Γ_{OH} vs absorbed sound intensity I_a, for $R_0 = 2$ μm bubbles. Circles: $f = 300$ kHz in Ar-sparged water. Square: the same but in 30%O_2/Ar-sparged water. Diamond: $R_0 = 2$ μm bubbles sonicated at 20 kHz in Ar-sparged water. The horizontal solid line corresponds to $\Gamma_{OH} = 2 \times 10^{17}$ molecules/J, an average value generally applicable to standard laboratory conditions.

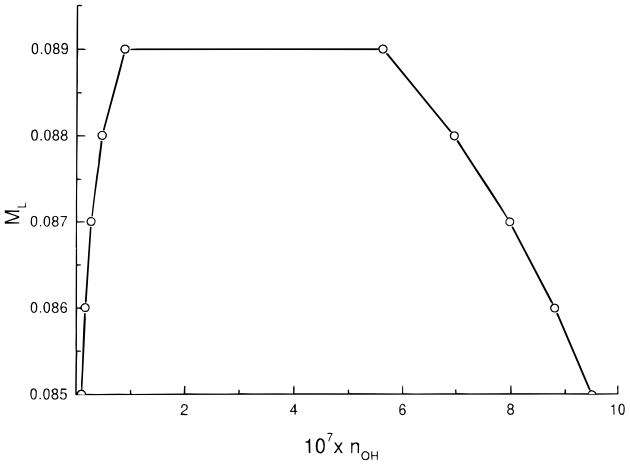

Figure 10. M_L vs n_{OH} parametric plot for the data of Figure 9. The end of collapse is actually a plateau rather than a point, over which n_{OH} varies 6.4 times.

corresponds to the median of the Blake radius: $R_B = 0.77\sigma/P_a = 0.24$ μm, and $R_0 = R_{max}/3 = 3.3$ μm, the requisite for transient cavitation.[4,14a,b] It is apparent that for any similar solute primary decomposition rates are uniquely determined by the acoustic frequency f, intensity I_a, power density Π, Henry's constant H, T, and $\langle R_0 \rangle$ for bubbles undergoing transient cavitation under such conditions. Net rates may be smaller than those calculated along these lines in the unlikely, but possible, case that the solute contained in the bubble fails to be consumed in a single collapse. Larger rates will be attained for solutes prone to secondary radical attack, or in the case that additional solute is incorporated into the bubble during expansion.

Sonochemical reactions of nonvolatile solutes necessarily involve the free radicals produced in the pyrolysis of water vapor. The number of oxidizing radicals produced per unit compression work at $R'' = 0$,

$$\Gamma_{OH} = n_{OH}/W_{ext} \tag{39}$$

is of direct relevance to the analysis of experimental data on the oxidation of such species. In Figure 9, we show calculated Γ_{OH} values for $R_0 = 2$ μm bubbles sonicated at 300 kHz at different powers. A maximum of $\Gamma_{OH} \sim 3.7 \times 10^{17}$ molecules/J is attained at optimal power (2.32 atm or 1.8 W/cm^2). Yields vary roughly by a factor of 10 within 1 and 100 W/cm^2, but drop precipitously outside this range. In this context, it is important to realize that the energy efficiency for the generation of cavitating bubbles leading to the full decomposition of the CCl_4 vapors derived above may be actually an upper limit for the bubbles implicated in water dissociation. In fact, Figure 8 shows that although CCl_4 is more than 95% decomposed, the number of OH radicals is increasing exponentially by the time the Mach number attains its maximum value. The parametric plot of Figure 10 clearly exposes the uncertainties involved in the estimation of Γ_{OH}: during the brief interval ($\sim$1 ns) in which the external forces vanish and the bubble loses its integrity, the number of OH radicals increases 6-fold. Accordingly, calculated Γ_{OH} values are assumed to be uncertain by a factor of 2$-$3 due to this effect alone. Therefore, we assume an average value of $\Gamma_{OH} \sim 2 \times 10^{17}$ OH radicals/J at 300 kHz for the analysis of experimental data that may not have been obtained at optimal conditions (see below).

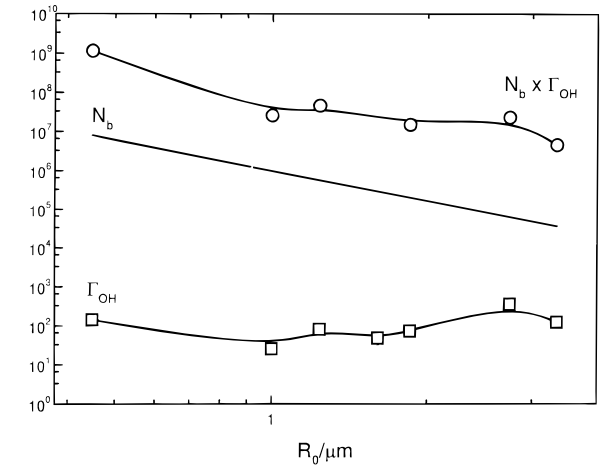

Figure 11. Squares: Γ_{OH} at (300 kHz, 1.8 W/cm^2). Solid line: the assumed equilibrium bubble size distribution function $N_b \propto R_0^{-3}$. Circles: the product ($N_b \times \Gamma_{OH}$) vs R_0, the equilibrium bubble radius.

Since actual experiments also reflect a distribution of bubble sizes, we investigated the dependence of Γ_{OH} on R_0 at optimal power (Figure 11). Our calculations span the range bracketed by $R_0 = 0.5$ μm (i.e, the Blake radius at $P_a = 2.3$ atm), and $R_0 = 3$ μm (i.e., $R_0 \sim R_{max}/3$, see above).[4,14a,b] We find that Γ_{OH} varies between 2.6×10^{16} and 3.5×10^{17} molecules/J in this interval. Assuming a steady-state bubble size distribution function of the form $N(R_0) \propto 1/R_0^3$ (i.e., similar to the one proposed by Gavrilov),[29] the expression

$$\langle \Gamma_{OH} \rangle = [\int_{0.5}^{3} \Gamma_{OH} N(R_0)\, dR_0]/[\int_{0.5}^{3} N(R_0)\, dR_0] \tag{40}$$

provides the desired average: $\langle \Gamma_{OH} \rangle = 1.3 \times 10^{17}$ molecules/J. Therefore, we estimate that in argon-saturated water OH radicals are generated at rates given by $r_{+OH} \sim 2 \times 10^{17}(1.3/3.7)\Pi = 3.5 \times 10^{15}$ molecules cm^{-3} s^{-1} $= 350 \pm 200$ μM min^{-1} at $\Pi = 0.05$ W/cm^3. The fact that this value—which is actually an upper limit because it applies in the absence of dissipation mechanisms such as heat transfer, viscosity effects, and post-collapse radical recombination reactions[12,14,30]—lies within a factor of 3 of typical experimental rates for the oxidation of iodide in this system is very significant.[16,17]

Before dealing with the dependence of Γ_{OH} yields on energy losses it is essential to consider the related issue of the extent of radical recombination following bubble breakup. To this end

we performed exponential adiabatic expansions on gas mixtures starting at R_{min} (i.e., the R value at $R'' = 0$) according to $R = R_{min}\{1 + A[1 - \exp(-t/\tau)]\}$, $T = T_{max}(R_{min}/R)^{3(\gamma-1)}$, with $1 + A = 100$, and variable time constants τ. For example, the excitation of a $R_0 = 2$ μm bubble by a (300 kHz, 1.8 atm) acoustic wave to $R_{max} = 6.67$ μm, followed by implosion, leads to the formation of $n_{OH} = 8.8 \times 10^7$, $n_O = 6.2 \times 10^5$, $n_H = 9.1 \times 10^6$, $n_{H2} = 4.0 \times 10^7$, and $n_{H2O2} = 2.3 \times 10^3$ molecules/bubble at $R_{min} = 1.15$ μm, $T_{max} = 4017$ K, $M_L = 0.089$. Notice the relatively small O and H atom yields. Expansion of this gas mixture with $\tau > 1$ μs results in $n_{O2}/(n_{H2O2} + 0.5n_{OH})$ ratios consistently exceeding 0.1, at variance with Hart and Henglein's findings.[16] *In other words, simultaneous gas expansion and cooling with time constants much longer than* $\tau \sim 3$ μs *necessarily lead to the conversion of OH radicals into* ($H_2 + O_2$) *via* H_2O_2 *and* HO_2 *as intermediate species*. On the other hand, there is little recombination, if any, for $\tau \leq 1$ μs. Actually we obtain $n_{OH} = 1.9 \times 10^8$ and $n_{H2} = 1.1 \times 10^8$ after adiabatic expansion and cooling to $T = 300$ K with $\tau = 1$ μs, which are about 2-fold larger than the initial values at R_{min}, indicating that water dissociation is not at chemical equilibrium at the end of collapse and proceeds even in the early stages of the "cooling" phase. The implications are that (1) the composition of the gas mixture after collapse is largely preserved during its dispersion into the liquid and (2) radicals may undergo recombination while competing with radical−molecule reactions only after they have been cooled and released into the solution. In the latter case, *all* atom and radical associations are expected to take place at diffusion-controlled rates, with rate constants $k \sim 6 \times 10^9$ M^{-1} $s^{-1} = 1 \times 10^{-11}$ cm^3 (molecule $s)^{-1}$ at 300 K.[31]

Heat and Mass Transfer Effects on Cavitation. While relatively minor, heat and mass transfer losses modulate chemical yields on account of the exponential dependence of rates on temperature. To test the possible effects, we adopted the equilibrium value of $\alpha = 7 \times 10^{-3}$ derived above for H_2O at 300 K, instead of $\alpha = 1 \times 10^{-3}$ as in the preceding calculations, and used ϵ as an adjustable parameter to fit Γ_{OH} yields to experimental I^- oxidation rates at 300 kHz. For example, we calculate an optimal value of $\Gamma_{OH} \sim 1 \times 10^{17}$ molecules/J at 300 kHz, $P_a = 2$ atm, with ($\alpha = 1 \times 10^{-3}$, $\epsilon = 0.03$) or, alternatively, with ($\alpha = 7 \times 10^{-3}$, $\epsilon = 0.04$) (cf., with the $\Gamma_{OH} \sim 3.7 \times 10^{17}$ molecules/J value derived above), a figure that brings estimates of sonochemical oxidative power in close agreement with experimental rates on iodide oxidation. Notice that, although the relative mass losses $\Delta n_{H2O}/n_{H2O}(0)$ increase with α from 5% to 27% in the range studied, we obtain similar OH-yields for both sets of parameters. Heat losses, $H_t/W_{ext} \sim$ 8%, are, of course, nearly identical in both cases. In Figure 12 we show mass and heat losses calculated for a typical collapsing bubble. It is apparent that integrated mass losses increase almost exponentially with time and that about 70% of the thermal losses into the surroundings take place in the last tenth of the bubble lifetime, when the temperature rises more than exponentially. Therefore, few radicals, which are precisely generated under the latter conditions, escape from the bubble *during* collapse.

The reason for these results is that the drier mixture gets hotter; that is, less H_2O dissociates more extensively leaving Γ_{OH} almost unchanged. This compensation effect holds within limits, however. Thus, our model predicts that with $\alpha \sim \epsilon \sim$ 0.1 mass losses will reach 95%, terminal temperatures will rise up to 14 700 K, and Γ_{OH} will drop about 4 orders of magnitude. Under such conditions OH radicals completely dissociate into H and O atoms that will rapidly escape into the solution unscathed or after undergoing all possible radical−radical and

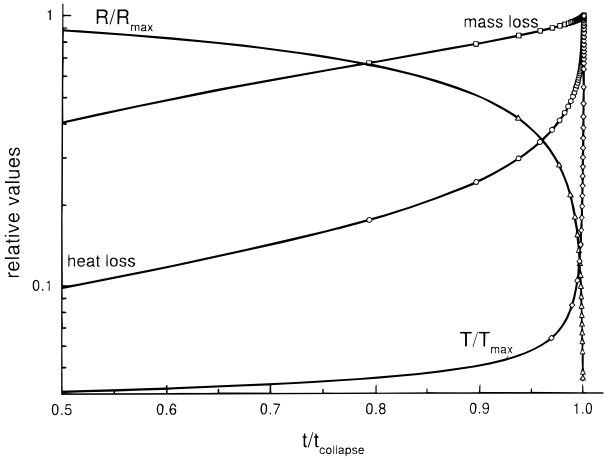

Figure 12. Relative mass (squares) and heat (circles) losses in a collapsing bubble. Absolute values depend on the actual accommodation coefficients α and ϵ (see text).

radical−molecule reactions (Table 1) in the expanding gas mixture (see above). We found that any OH radicals formed in the latter process will preferentially dimerize into H_2O_2 rather than engage in the slower atom−radical association reactions. The ultimate fate of H_2O_2 is, however, to undergo radical attack yielding ($H_2 + O_2$), at variance with Hart and Henglein's experimental observations[16] and Hua and Hoffmann's measurements on OH-trapping by terephthalic acid.[18] On the other hand, if O and H atoms escape directly into the liquid their diffusion-controlled association reactions—lacking the energy relaxation restrictions prevalent in the gas phase—become competitive with OH radical dimerization and will generate substantial O_2 yields as well.[31] In other words, although there is some latitude regarding the precise values of accommodation coefficients,[32] chemical evidence seems to rule out values larger than $\alpha \sim$ 0.01 (see Appendix 1). The implication is that the bubbles involved in sonochemistry are largely filled with water vapor, and their temperatures never exceed 10 kK. As commented above, there are no chemical restrictions on maximum temperatures within a small core heated by incident shock waves. Such waves may develop under certain conditions that are not entirely unrelated to the chemistry occurring prior to the onset of shock phenomena.

This analysis would not be complete without pointing out that there is evidence that milder events occur along hard collapses, as suggested by the fact that experimental ozone decomposition rates are about 10-fold larger than those estimated based on its Henry's constant and applied power.[28,33] It can be shown that the relatively low temperatures required by the exothermic decomposition of labile O_3 can be attained even in periodic bubble oscillations, a process whose energy requirements are minimal.

Conclusions

A realistic dynamic analysis of bubble motion that conserves all forms of energy along the course of transient cavitation accounts for observed sonochemical effects. Chemical enthalpy changes in the reacting vapor are an integral part of this analysis. The work performed on the vapor and the attending pressure and temperature changes do not generally correspond to those calculated for the adiabatic compression of an unreactive gas. The transfer of mass and heat across the bubble wall is explicitly incorporated into the model as discrete kinetic processes characterized by specific accommodation coefficients. Chemical evidence suggests that neither process is extensive but, while

mass transfer largely takes place in the initial stages of collapse, $R_0 < R < R_{max}$, heat is mostly transferred shortly before rebound. By assuming that spherical bubbles become unstable and break up (thereby dispersing their content into the liquid) when the radial acceleration vanishes, we are able to estimate absolute sonochemical degradation rates of volatile solutes and oxidation rates of nonvolatile solutes that are in good agreement with reported experimental data. These calculations identify the relevant parameters—such as ultrasound frequency, intensity (W m^{-2}), and power density (W m^{-3})—required for the proper assessment and comparison of sonochemical experiments.

Acknowledgment. A.J.C. is a visiting scientist, on leave from the University of Buenos Aires and the National Research Council of Argentina. Financial support from Advanced Research Projects Agency, ARPA (Grant NAV5HFMN N0001492J1901), the Office of Naval Research, ONR, the Electric Power Institute, EPRI (Grant RP 8003-37), and the Department of Energy, DOE/Argonne, Grant 1963472402, is gratefully acknowledged. We thank the reviewers for valuable comments.

Appendix 1

Let us try to isothermally contract a bubble from R_{max} to R_0 maintaining the equilibrium water vapor density δ in its interior during the half-period [$t_{1/2} = 10^3/(2f)$] of an acoustic wave of frequency f kHz. The total number N of water molecules to be removed is $N = 4.19(R_{max}^3 - R_0^3)\delta$. The instantaneous rate of water losses in collisions with the bubble wall is given by dn/dt(molecules/s) $= (1/4)\delta\langle c\rangle\alpha 4\pi R^2 = 1.85 \times 10^{-3}\alpha R^2\delta$ (R in μm) at 300 K. Without loss of generality, we evaluate an average rate by assuming that $\langle R^2\rangle \sim (R_{max}^2 + R_0^2)/2$. Therefore, only if

$$\alpha \geq 9.1 \times 10^{-6} f R_0 (Z - 1)/(Z^{2/3} + 1) \qquad (41)$$

is it possible to accomplish the task. At $f = 300$ kHz, with $Z = (R_{max}/R_0)^3 = 1.73$, $R_0 = 2$ μm, we get $\alpha \geq 1.6 \times 10^{-3}$. For $\alpha = 7 \times 10^{-3}$, the upper limit derived in the text, it is feasible to dispose of the vapor contained in a bubble expanded to $R_{max}/R_0 \sim 2$. In other words, the adopted α values are sufficient to maintain liquid−vapor equilibrium in periodic bubble oscillations of moderate amplitude at 300 kHz. Since $R_{max} \propto 1/f$ (cf. eq 36), the latter condition is only weakly dependent on f. However, δ will inevitably increase during compression at the larger expansion ratios $R_{max}/R_0 \geq 3$ required for transient cavitation, regardless of the extent of equilibration in the preceding expansion phase. This phenomenon is generally compounded by the increasingly shorter compression times in the train of unsymmetric oscillations leading to the final collapse event. As a result, late expansions will take place in oversaturated bubbles. This hysteresis effect is akin but not identical to bubble growth via rectified diffusion of permanent gases.[14b] Notice that, although vaporization and condensation rates are related by detailed balance under any (including nonequilibrium) conditions,[34] condensation rates during collapse and vaporization rates on prior expansions are *not*. In other words, it is possible to be closer to equilibrium during expansion than during compression at large R_{max}/R_0 ratios. Thus, only if collapse events were reversible or set by a single expansion stage would it be necessary to call for larger α values to ensure equilibrium vapor pressures at the onset of cavitation.

References and Notes

(1) Margulis, M. A., Ed. *Sonochemistry and Cavitation*; Gordon and Breach: Newark, NJ, 1995.

(2) Suslick, K. J., Ed. *Ultrasound, Its Chemical, Physical and Biological Effects*; VCH: Weinheim, Germany, 1988.

(3) Henglein, A. *Ultrasonics* **1987**, *25*, 6.

(4) Mason, T. J.; Lorimer, J. P. *Sonochemistry. Theory, Applications and Uses of Ultrasound in Chemistry*; Wiley: New York, 1988; Chapter 2. (b) Mason, T. J., Ed. *Advances in Sonochemistry*; JAI Press: New York, 1990−1994; Vols. 1−3.

(5) Bernstein, L. S.; Zakin, M. R. *J. Phys. Chem.* **1995**, *99*, 14619.

(6) Bernstein, L. S.; Zakin, M. R.; Flint, E. B.; Suslick, K. S. *J. Phys. Chem.* **1996**, *100*, 6612.

(7) Mišík, V.; Riesz, P. *Ultrasonics Sonochem.* **1996**, *3*, 25.

(8) Didenko, Y. T.; Pugach, S. P. *J. Phys. Chem.* **1994**, *98*, 9742.

(9) Lohse, D.; Hilgenfeldt, S. *J. Chem. Phys.* **1997**, *107*, 6986.

(10) Löfstedt, R.; Weninger, K.; Putterman, S.; Barber, B. P. *Phys. Rev. E* **1995**, *51*, 4400. (b) Barber, B. P.; Putterman, S. *Nature* **1991**, *352*, 318. (c) Hiller, R. A.; Putterman, S. *Phys. Rev. Lett.* **1995**, *75*, 3549.

(11) Ashokkumar, M.; Hall, R.; Mulvaney, P.; Grieser, F. *J. Phys. Chem.* **1997**, *101*, 10845.

(12) Kamath, V.; Oguz, H. N.; Prosperetti, A. *J. Acoust. Soc. Am.* **1992**, *92*, 2016. (b) Kamath, V.; Prosperetti, A.; Egolfopoulos, F. N. *J. Acoust. Soc. Am.* **1993**, *94*, 248.

(13) Rayleigh, Lord. *Philos. Mag.* **1917**, *34*, 94.

(14) a) Leighton, T. G. *The Acoustic Bubble*; Academic Press: London, 1994; pp 84−90. (b) *Ibid.*, pp 301−328.

(15) Brennen, C. E. *Cavitation and Bubble Dynamics*; Oxford University Press: New York, 1995; Chapter 2. (b) *ibid.*, chapter 3. (c) Flynn, H. G. *J. Acoust. Soc. Am.* **1975**, *58*, 1160.

(16) Hart, E. J.; Henglein, A. *J. Phys. Chem.* **1985**, *89*, 4342.

(17) Hua, I.; Hoffmann, M. R. *Environ. Sci. Technol.* **1997**, *31*, 2237.

(18) Hua, I.; Hoffmann, M. R. *Environ. Sci. Technol.* **1996**, *30*, 864.

(19) H.-M. Hung; Hoffmann, M. R. *Environ. Sci. Technol.*, submitted.

(20) NIST Chemical Kinetics Database 17, Version 5.0; Westley, F.; Frizzell, D. H.; Herron, J. T.; Hampson, R. F.; Mallard, W. G. National Institute of Standards and Technology, Gaithersburg, MD, 1993. (b) Baulch, D. L.; Cobos, C. J.; Frank, P.; Hayman, G.; Just, Th.; Murrells, T.; Pilling, M. J.; Troe, J.; Walker, R. W.; Warnatz, J. *J. Phys. Chem. Ref. Data*, **1994**, *23*, 847. See particularly the data on the (OH + OH + M) reaction, p 870.

(21) Tsang, W.; Hampson, R. F. *J. Phys. Chem. Ref. Data.* **1986**, *15*, 1087.

(22) Curtis, A. R.; Sweettenham, W. P. *FACSIMILE*; Harwell: U.K., 1987.

(23) Wu, C. C.; Roberts, P. H. *Phys. Rev. Lett.* **1993**, *70*, 3424.

(24) Suslick, K. S.; Mdleleni, M. M.; Ries, J. T. *J. Am. Chem. Soc.* **1997**, *119*, 9303.

(25) Prasad Naidu, D. V.; Rajan, R.; Kumar, R.; Gandhi, K. S.; Arakeri, V. H.; Chandrasekaran, S. *Chem. Eng. Sci.* **1994**, *49*, 877.

(26) Sochard, S.; Wilhelm, A. M.; Delmas, H. *Ultrasonics Sonochemistry* **1997**, *4*, 77.

(27) Hart, E. J.; Henglein, A. *J. Phys. Chem.* **1987**, *91*, 3654. (b) Gutiérrez, M.; Henglein, A.; Dohrmann, J. K. *J. Phys. Chem.* **1987**, *91*, 6687.

(28) Hart, E. J.; Henglein, A. *J. Phys. Chem.* **1986**, *90*, 3061.

(29) Gavrilov, L. R. In *Physical Principles of Ultrasonic Technology*; Plenum Press: New York, 1973; Vol. 2, Part VI. (b) Katz, J.; Acosta, A. *Appl. Sci. Res.* **1982**, *38*, 123. (c) Henglein, A.; Herburger, D.; Gutiérrez, M. *J. Phys. Chem.* **1992**, *96*, 1126. (d) Leighton, T. G. *Ultrasonics Sonochem.* **1995**, *2*, S125.

(30) Kondo, T.; Kirschenbaum, L. J.; Kim, H.; Riesz, P. *J. Phys. Chem.* **1993**, *97*, 522. (b) Riesz, P. In *Advances in Sonochemistry;* Mason, T. J., Ed.; Jai Press: Greenwich, CT, 1991; Vol 2, p 24. (c) Colussi, A. J.; Hoffmann, M. R. Unpublished results.

(31) Berry, S. R.; Rice, S. A.; Ross, J. *Physical Chemistry*; Wiley: New York, 1980; p 1159. (b) Ross, A. B.; Bielski, B. H. J.; Buxton, G. V.; Cabelli, D. E.; Greenstock, C. L.; Helman, W. P.; Huie, R. E.; Grodkowski, J.; Neta, P. *NDRL/NIST Solution Kinetics Database* 40, version 2.0; National Institute of Standards and Technology: Gaithersburg, MD, 1994.

(32) Nathanson, G. M.; Davidovits, P.; Worsnop, D. R.; Kolb, C. E. *J. Phys. Chem.* **1996**, *100*, 13007. The strong negative temperature dependence found for mass accommodation coefficients of thermalized polar species such as H_2O_2 on water suggests α values close to the assumed range for the probability of sticking hot H_2O molecules on water at room temperature.

(33) Weavers, L. K. Doctoral Dissertation, California Institute of Technology, 1997.

(34) Benson, S. W. *Thermochemical Kinetics*, 2nd ed.; Wiley: New York, 1976; p 3.